Available online at www.sciencedirect.com
ScienceDirect
Geochimica et Cosmochimica Acta 70 (2006) 4166–4180
Geochimica
www.elsevier.com/locate/gca

Reactive iron(III) in sediments: Chemical versus microbial extractions

C. Hyacinthe *, S. Bonneville, P. Van Cappellen

Department of Earth Sciences-Geochemistry, Faculty of Geosciences, Utrecht University, P.O. Box 80021, 3508 TA, Utrecht, The Netherlands

Received 11 August 2005; accepted in revised form 23 May 2006

Abstract

The availability of particulate Fe(III) to iron reducing microbial communities in sediments and soils is generally inferred indirectly by performing chemical extractions. In this study, the bioavailability of mineral-bound Fe(III) in intertidal sediments of a eutrophic estuary is assessed directly by measuring the kinetics and extent of Fe(III) utilization by the iron reducing microorganism *Shewanella putrefaciens*, in the presence of excess electron donor. Microbial Fe(III) reduction is compared to chemical dissolution of iron from the same sediments in buffered ascorbate-citrate solution (pH 7.5), ascorbic acid (pH 2), and 1 M HCl. The results confirm that ascorbate at near-neutral pH selectively reduces the reactive Fe(III) pool, while the acid extractants mobilize additional Fe(II) and less reactive Fe(III) mineral phases. Furthermore, the maximum concentrations of Fe(III) reducible by *S. putrefaciens* correlate linearly with the iron concentrations extracted by buffered ascorbate-citrate solution, but not with those of the acid extractions. However, on average, only 65% of the Fe(III) reduced in buffered ascorbate-citrate solution can be utilized by *S. putrefaciens*, probably due to physical inaccessibility of the remaining fraction of reactive Fe(III) to the cells. While the microbial and abiotic reaction kinetics further indicate that reduction by ascorbate at near-neutral pH most closely resembles microbial reduction of the sediment Fe(III) pool by *S. putrefaciens*, the results also highlight fundamental differences between chemical reductive dissolution and microbial utilization of mineral-bound ferric iron.

1. Introduction

Changes in the redox state of iron have a major impact on the biogeochemical cycling of carbon, sulfur, nitrogen, phosphorus and (trace) metals (Haese et al., 1998). Under suboxic conditions, ferric iron is a potential electron acceptor for organic matter degradation (Froelich et al., 1979; Lovley and Phillips, 1988), and studies in freshwater (Jones et al., 1983; Jones et al., 1984; Lovley and Phillips, 1986a,b; Roden and Wetzel, 1996) and marine (Canfield, 1993; Thamdrup et al., 1994; Thamdrup, 2000; Jensen et al., 2003) habitats indicate that dissimilatory Fe(III) reduction can contribute substantially to the oxidation of organic compounds. *In situ* dissimilatory iron reduction is influenced by a variety of factors, including the microbial community structure and biomass (Dollhopf et al., 2000), the quality and quantity of the organic matter (Chen et al., 2003), and the type and abundance of Fe(III) minerals (Bonneville et al., 2004).

Due to its low solubility, Fe(III) tends to accumulate in particulate form, mostly as ferric (hydr)oxides (Murray, 1979), Fe(III) bound in alumino-silicates (Raiswell and Canfield, 1998), and ferric phosphate phases (Buffle et al., 1989; Hyacinthe and Van Cappellen, 2004). The speciation and reactivity of particulate iron in soils and sediments are generally inferred using chemical extractions (Chao and Zhou, 1983; Canfield, 1988; Slomp et al., 1997). Although these methods are based on an indirect identification of the minerals involved, they are simple to implement and are able to detect small amounts of poorly crystalline phases, which may be difficult to quantify using spectroscopic techniques. Furthermore, some of the limitations of single-step extractions can be overcome by performing kinetic extractions, in which the release of iron and other elements by a given extractant is followed as a function of time. Kinetic extractions provide a more complete characterization of the composition and chemical reactivity of iron pools in

* Corresponding author. Fax: +31 30 253 5302.
E-mail address: C.Hyacinthe@geo.uu.nl (C. Hyacinthe).

0016-7037/$ - see front matter © 2006 Elsevier Inc. All rights reserved.
doi:10.1016/j.gca.2006.05.018

natural samples (Postma, 1993; Larsen and Postma, 2001; Ferro, 2003; Hyacinthe and Van Cappellen, 2004).

Particulate Fe(III) in soils and sediments exhibits highly variable mineralogy, crystallinity, grain size and impurity content. This heterogeneity affects its chemical reactivity and, most likely, its availability to iron reducing microorganisms. Rates of chemical dissolution, however, cannot be directly related to *in situ* rates of dissimilatory Fe(III) reduction, because factors in addition to mineral reactivity affect the activity of the iron reducers (Roden, 2004). Hence, till now, studies have either focused on the chemical reactivity of particulate Fe(III), or on the ecological and environmental controls of dissimilatory iron reduction, with only a few studies linking the results of chemical extractions directly to Fe(III) bioavailability (Lovley and Phillips, 1986a; Hacherl et al., 2001; Roden and Wetzel, 2002; Roden, 2004).

In this paper, we compare chemical and microbial iron extractions of freshwater and brackish sediments collected along the eutrophic Scheldt estuary (Belgium and the Netherlands). Previous studies have shown that the sediments are enriched in authigenic Fe(III) phases (Hyacinthe and Van Cappellen, 2004), and contain diverse populations of iron reducing microorganisms (Lin, 2006).

To assess the chemical reactivity of the sedimentary iron pools, we performed kinetic leaching experiments with three extractants commonly used in the field of iron geochemistry: ascorbate-citrate solution buffered at pH 7.5, ascorbic acid, and 1 M HCl (Chao and Zhou, 1983; Canfield, 1988; Svendsen et al., 1993; Kostka and Luther, 1994; Raiswell et al., 1994; Haese et al., 1998; Poulton and Raiswell, 2005). The selected extractants dissolve iron associated with relatively reactive mineral phases, but the dissolution mechanisms differ markedly, from purely reductive dissolution to proton-promoted, non-reductive dissolution (Dos Santos Afonso et al., 1990; Hering and Stumm, 1990; Stumm and Sulzberger, 1992). Furthermore, the acid extractions may mobilize ferric as well as ferrous iron phases (Cornwell and Morse, 1987; Haese et al., 1998).

For the microbial extractions, we used *Shewanella putrefaciens*, a facultative anaerobic Gram negative bacterium, which can substitute Fe^{3+} for O_2 as terminal electron acceptor in respiration (DiChristina and DeLong, 1994). The organism is known to reduce Fe(III) (hydr)oxide minerals, including hydrous ferric oxide (HFO), goethite, hematite and magnetite (Nealson and Saffarini, 1994; Roden and Wetzel, 1996; Fredrickson et al., 1998; Zachara et al., 1998), Fe(III) present in natural sediments (Fredrickson et al., 1998; this study), and structural Fe(III) bound in clay minerals (Kostka et al., 1999). Therefore, it was used as a model microorganism to probe the microbial reactivity and potential availability of sedimentary Fe(III). In addition to quantifying differences in microbial reduction kinetics, an important goal was to determine the bioavailability of Fe(III) in the sediments, under conditions where neither the biomass of iron reducers nor the electron donor were limiting.

2. Materials and methods

2.1. Sediments

Sediment cores were collected in the unvegetated parts of two intertidal marshes along the Scheldt estuary, a well-studied macrotidal estuary in NW Europe (Baeyens et al., 1998; Wollast, 1988). The sites, Appels and Waarde, are respectively, 127 and 40 km upstream from Vlissingen, where the estuary flows into the North Sea. The freshwater marsh at Appels is located in the outside bend of a meander of the tidally-influenced Scheldt river, while the Waarde marsh is in the brackish part of the lower estuary. A complete description of the sites, a map with their locations, and the sampling techniques can be found in Hyacinthe and Van Cappellen (2004).

At both sites, three cores were taken in close proximity to each other and sliced under anaerobic conditions. The following six depth intervals were used in this study: 0–1 cm (A0–1), 13–15 cm (A13–15) and 39–41 cm (A39–41) for Appels, and 0–1 cm (W0–1), 13–15 cm (W13–15) and 33-35 cm (W33–35) for Waarde. The corresponding sediment slices in each of the three cores were combined, homogenized and kept at 5 °C under anaerobic conditions during transport to the laboratory (approximately 2 h). Sediment dedicated to the different chemical extractions was stored without any further treatment at −30 °C, while sediment for the microbial incubations was freeze-dried. Sampling, freeze-drying and storage were performed under inert atmosphere (Ar), in order to prevent oxidation artifacts.

Note that the sediments used in the microbial experiments were freeze-dried, rather than autoclaved. Freeze-drying is the preferred method to preserve the solid-state speciation and oxidation state of iron (Bordas and Bourg, 1998), as autoclaving is known to modify hydrous and amorphous iron minerals (Schwertmann and Cornell, 1991). Because freeze-drying does not necessarily kill the microorganisms present in the sediments, control experiments were performed to determine whether any surviving autochtonous organisms contributed to the observed iron reduction in the microbial extractions (Section 2.3).

2.2. Chemical extractions

Kinetic extraction experiments of the sediments were carried out in a 500 mL cylindrical reactor, at 25 ± 0.3 °C and in the dark. For each experiment, 350 mL of anoxic extraction solution (Table 1) was prepared. At time zero, 15 mL of freshly thawed sediment was added with a syringe. The suspension was stirred by a suspended stir bar and continuously purged with argon, for the 24 h duration of the experiments. During the 24 h of experiment, pH was continuously monitored and only minor pH changes were observed in all three extractions. Filtered samples (0.2 μm pore size) were periodically collected with a syringe connected to a three-way valve situated at the bottom of the

Table 1
Chemical extractions

Extraction	Extractant preparation	References
Buffered ascorbate	Sodium citrate (50 g/L) + sodium bicarbonate (50 g/L) One hour bubbling with N_2 20 g/L of L(+)ascorbic acid pH 7.5	Ferdelman, 1988; Kostka and Luther, 1994; Ferro, 2003; Hyacinthe and Van Cappellen, 2004
Ascorbic acid	20 g/L of L(+)ascorbic acid pH 2	Postma, 1993; van der Zee and van Raaphorst, 2004
1 M HCl	HCl supra pur	Chao and Zhou, 1983; Canfield, 1988; Slomp et al., 1997

reactor. The aliquots were immediately acidified upon retrieval to prevent oxidation and later analyzed for iron and other major elements by ICP/OES. A complete description of the reactor and experimental protocol can be found in Hyacinthe and Van Cappellen (2004).

Additional kinetic extraction experiments with single Fe(III) mineral phases were carried out in buffered ascorbate–citrate solution. Ferric phosphate was synthesized by neutralizing a solution composed of $FeCl_3 \cdot 6H_2O$ (0.2 M) and K_2HPO_4 (0.2 M) with NaOH. To remove the K^+ and Cl^- ions, the suspension was dialyzed with demineralized water adjusted to neutral pH. The solid consisted of amorphous nanoparticles with a molar P/Fe ratio of 0.77. Lepidocrocite and coarse-grained hematite were purchased from Scholz (for more details on these oxides, see, Bonneville et al., 2004). The release of Fe^{2+} to solution was monitored as a function of time in 0.25 g L^{-1} suspensions of lepidocrocite and hematite, and a 0.15 g L^{-1} suspension of ferric phosphate. All other experimental conditions were identical to the kinetic extractions with the natural sediments. However, because of relatively slow dissolution, the experiments with lepidocrocite and hematite lasted for one month.

The time-dependent release of iron to solution was fitted to the reactive continuum model (Boudreau and Ruddick, 1991; Postma, 1993; Koning et al., 1997; Larsen and Postma, 2001; Ferro, 2003; Hyacinthe and Van Cappellen, 2004; van der Zee and van Raaphorst, 2004):

$$\frac{J}{M(0)} = \frac{\upsilon}{a}\left(\frac{M(t)}{M(0)}\right)^{1+\frac{1}{\upsilon}} \quad (1)$$

where J, υ/a and $1 + 1/\upsilon$ are the dissolution rate (μmol g^{-1} s^{-1}), apparent rate constant (s^{-1}), and apparent reaction order, respectively. $M(0)$ stands for the initial mass of extractable iron present in the sediment sample, and $M(t)$ is the corresponding mass remaining at time t. Rate Eq. (1) assumes that the initial mineral assemblage exhibits a continuous reactivity distribution described by a gamma function (Boudreau and Ruddick, 1991). The resulting time evolution of $M(t)$ is then given by:

$$M(t) = M(0)\left(\frac{a}{a+t}\right)^{\upsilon} \quad (2)$$

Under the far-from-equilibrium conditions of the experiments, the apparent rate constant, υ/a, equals the initial, mass-normalized, dissolution rate and, hence, allows one to directly rank the relative kinetic efficiencies of the three extraction solutions. The exponent in the rate equation, $1 + 1/\upsilon$, is a measure of the heterogeneity of the mineral assemblage undergoing dissolution. For a homogeneous reactivity the apparent reaction order approaches one, while values exceeding one are indicative of a distribution of reactivities.

Optimized values of the parameters υ, a and $M(0)$ were determined by fitting the time-dependent dissolution data to Eq. (2), using the Matlab statistics toolbox. Note that, experimentally, $M(t)$ was obtained by subtracting from $M(0)$ the amount of iron that had accumulated in solution at a given time. In addition to the optimized parameter values, lower and upper limits were obtained for the 95% confidence intervals.

2.3. Microbial extractions

Cultures of *Shewanella putrefaciens* 200R (DiChristina and DeLong, 1994; DiChristina et al., 2002) were maintained frozen within glycerol in the presence of rifamycin. For the experiments, frozen cells were revitalized on agar plates in Luria–Bertani (LB) medium (Bertani, 1951). Single colonies from plates were inoculated into 50 mL LB medium and harvested in middle exponential phase (Optical Density at 660 nm, OD = 0.4). (Note: optical densities were calibrated by direct cell counts using epifluorescence microscopy, following Hobbie et al., 1977). Aliquots of harvested cells were distributed over 4 bottles of 150 mL LB medium, and the cells were allowed to grow again for 12 h under aerobic conditions to middle exponential phase. The cells were then washed three times with sterile salt solution (10 mM Hepes buffer, 28 mM NH_4Cl, 1 mM $CaCl_2 \cdot 2H_2O$, pH 7) and concentrated by centrifugation for use in the incubations. In all experiments the initial pH of the reaction medium was adjusted to 7 using sterile NaOH or HCl solutions, prior to introducing the cells.

A first series of experiments was conducted to assess the possible effects of autochtonous microorganisms and lactate addition on ferrous iron production. For four of the six depth intervals (A0–1, A39–41, W0–1 and W33–35), 2 g of freeze-dried sediment was mixed with 100 mL of sterile salt medium, amended or not with lactate and *S. putrefaciens*. The following four combinations were tested: (1)

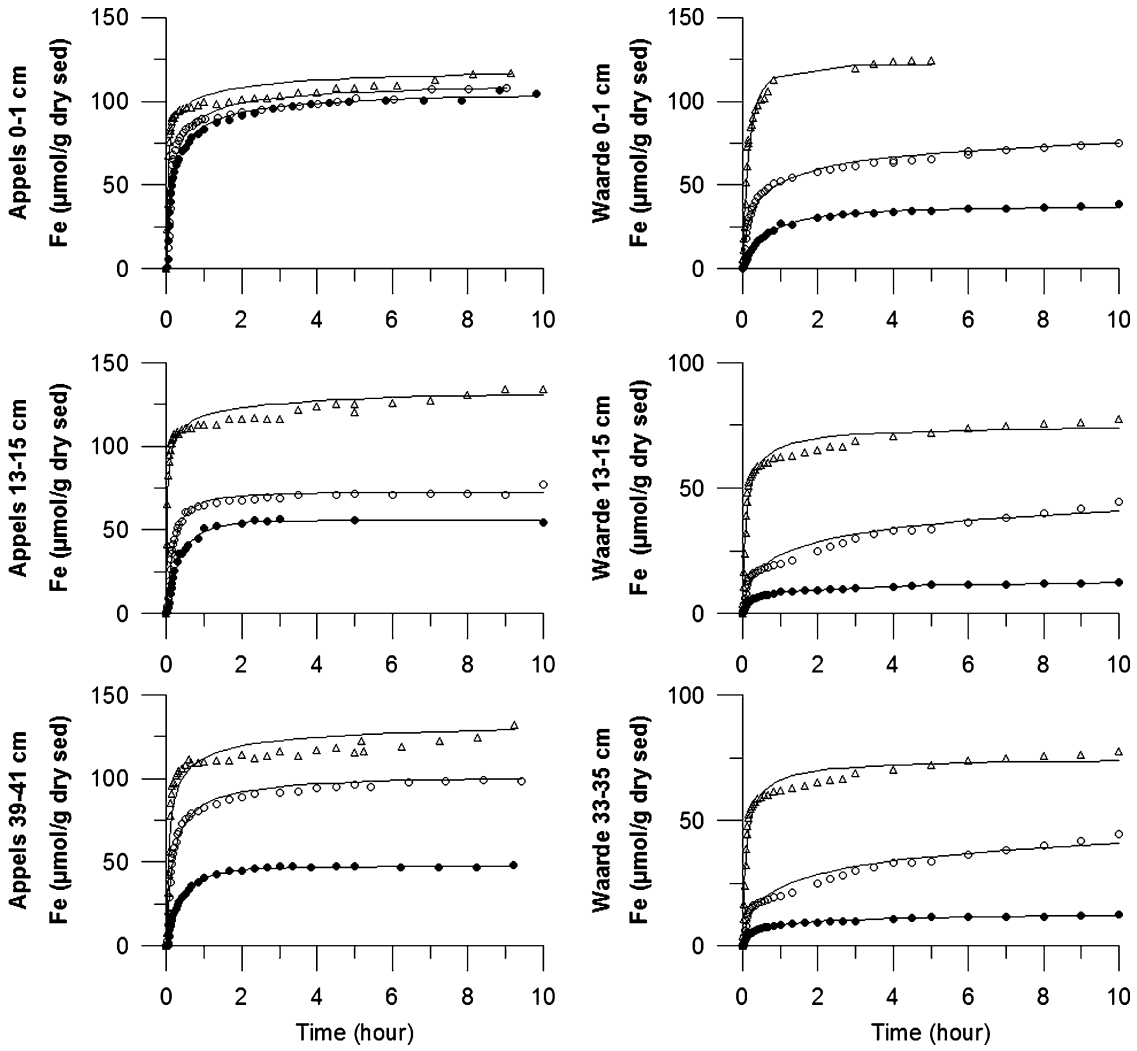

Fig. 1. Dissolution of iron from the sediments of Appels and Waarde as a function of time, for the three chemical extractions (buffered ascorbate = filled circles, ascorbic acid = open circles, HCl = triangles). The lines represent the best fits of the reactive continuum model to the data. See text for complete discussion.

salt medium alone, (2) salt medium plus 10 mM lactate, (3) salt medium plus *S. putrefaciens* ($5.9 \pm 0.8 \times 10^{11}$ cells L^{-1}), and (4) salt medium plus 10 mM lactate and *S. putrefaciens* ($5.9 \pm 0.8 \times 10^{11}$ cells L^{-1}).

In the second series of experiments, kinetic parameters describing the reduction of sedimentary Fe(III) by *S. putrefaciens* in the presence of excess electron donor were determined. For each of the six depth intervals, 0.5 to 50 g of freeze-dried sediment was suspended together with a fixed cell density of *S. putrefaciens* ($2.1 \pm 0.2 \times 10^{11}$ cells L^{-1}) in 100 mL of sterile salt solution amended with lactate (10 mM). The incubations were carried out at 25 ± 1 °C in airtight bottles with argon filled headspaces. They lasted for 600 h.

In the third series of experiments, freeze-dried sediment from each of the six depth intervals was first extracted with ascorbate-citrate solution at pH 7.5 for 24 h. After centrifugation and removal of the supernatant, the sediment was resuspended in lactate amended (10 M) sterile salt medium in the presence of *S. putrefaciens* ($1.9 \pm 0.3 \times 10^{11}$ cells L^{-1}). The incubations were carried out in exactly the same manner as those in the previous series of experiments.

The suspensions in the reaction bottles were periodically sampled, and iron reduction was quantified by monitoring the build-up of dissolved plus adsorbed ferrous iron. Dissolved ferrous and ferric iron concentrations were measured, after sample filtration (0.2 µm pore size) and acidification, following the method of Viollier et al. (2000). Adsorbed Fe^{2+} was measured using a modified ferrozine extraction method (Stookey, 1970; Sorensen, 1982; van der Zee, 2002). The ferrozine extraction solution consisted of 10 mL monosodium salt hydrate of (3-(2-pyridyl)-5,6-bis-(4-phenylsulfonic acid)-1,2,4 triazine)*p-p'*-disulfonic acid (5 g L^{-1}), ammonia acetate (4 g L^{-1}), 10 mL of ammonium acetate (5 M) solution adjusted to pH 9.5 with ammonium hydroxide (28–30% NH_4OH), and diluted to a final volume of 100 mL with ultrapure

water. Aliquots of 0.5 mL of suspension were extracted with 5 mL of the ferrozine solution for 20 min. After centrifugation, the Fe^{2+} concentration in the supernatant was measured spectrophotometrically at 562 nm wavelength.

3. Results

3.1. Chemical extractions

Iron dissolution curves in the three different extraction solutions are plotted in Fig. 1 for the sediments from Appels and Waarde. Also shown on the figure are the best fits of the reactive continuum model to the data. Although Fig. 1 only presents Fe^{2+} produced during the first 10 h of the extractions, Eq. (2) was fitted to the data collected over the entire duration of the experiments (24 h). The corresponding fitted model parameters are given in Table 2.

Iron release from the sediments resulted in a rapid build-up of dissolved Fe^{2+} within the first half hour, followed by a decelerating production of Fe^{2+} (Fig. 1). For any given sample, the initial Fe^{2+} release was fastest in 1 M HCl and slowest in buffered ascorbate solution. The final concentrations of iron, phosphorus and calcium dissolved from the sediments after 24 h are listed in Table 3.

The reactive continuum model provided near-perfect fits to the iron dissolution curves in buffered ascorbate–citrate solution, with correlation coefficients (r^2) on the order of 0.99. Not only were the correlation coefficients lower for the two other extractions ($r^2 \leqslant 0.95$), but the model fits systematically deviated from the observed dissolution curves: initial iron dissolution during the first 30 min was generally underpredicted, while subsequent iron release was overpredicted over the next few hours (Fig. 1). The deviations were more pronounced for the HCl than the ascorbic acid extractions. Nonetheless, in agreement with the visual inspection of the initial parts of the dissolution curves, the fitted apparent rate constants, υ/a, increased in the order: buffered ascorbate (pH 7.5) < acid ascorbic (pH 2) < HCl (1 M).

The lowest apparent reaction orders, $1 + 1/\upsilon$, were obtained for the two deeper sediment samples of Appels extracted in ascorbate-citrate solution at pH 7.5 (Table 2). In a previous study, this extractant systematically yielded values of $1 + 1/\upsilon$ approaching one for Appels sediments, suggesting that a relatively homogeneous iron pool was extracted (Hyacinthe and Van Cappellen, 2004). As also observed in this earlier study, buffered ascorbate extractions of Waarde sediments yielded reaction orders significantly higher than one. The main difference with our previous results was the relatively high value of $1 + 1/\upsilon$ (2.5) for the buffered ascorbate extraction of the topmost sediment at Appels. For the 1 M HCl and pH 2 ascorbic acid extractions, apparent reaction orders varied between 1.4 and 6.0, with no discernible trends.

The concentrations of total extractable iron, $M(0)$, obtained by fitting Eq. (2) to the dissolution curves agreed well with the dissolved iron concentrations measured at the end of the extractions (Tables 2 and 3). As can be seen from the tables, $M(0)$ values increased in the order: buffered ascorbate < acid ascorbic < HCl. The exception was the uppermost sample of Appels, where the three extractions released similar iron concentrations (≈110 μmol Fe g^{-1} dry sediment). This sample also exhibited the highest concentration of buffered ascorbate extractable iron of all the sediment samples studied.

Buffered ascorbate–citrate extractions released more iron from the Appels than the Waarde sediments. The 1 M HCl extractions, however, yielded comparable $M(0)$ values at both sites. The three extractions showed contrasting depth dependencies. For example, at Appels, iron

Table 2
Reactive continuum model parameters for the chemical extractions of the estuarine sediments

	(υ/a) (10^{-4} s^{-1})	$(1 + 1/\upsilon)$	$M(0)$ (μmol/g dry sed)
A0–1 asc7	16.8 (19.3–15.6)	2.5 (3.0–2.2)	109 (112–105)
A13–15 asc7	7.7 (14.7–7.4)	1.3 (3.3–1.1)	56.0 (57.3–54.8)
A39–41 asc7	7.6 (8.7–7.3)	1.3 (1.6–1.2)	47.4 (48.0–46.8)
W0–1 asc7	4.6 (4.8–4.4)	1.8 (2.0–1.6)	38.1 (38.8–37.4)
W13–15 asc7	13.8 (16.1–12.9)	4.3 (6.2–3.5)	23.5 (26.3–20.7)
W33–35 asc7	8.9 (9.3–8.7)	4.9 (7.0–3.9)	17.2 (19.5–14.9)
A0–1 asc2	19.6 (27.9–17.3)	2.5 (3.3–2.1)	113 (118–107)
A13–15 asc2	14.4 (17.3–13.5)	1.5 (1.9–1.4)	72.5 (73.7–71.3)
A39–41 asc2	16.8 (20.2–15.3)	2.3 (2.8–2.0)	104 (107–101)
W0–1 asc2	9.5 (9.5–9.4)	6.0 (10.0–4.5)	117 (141–92)
W13–15 asc2	21.4 (44.3–18.7)	2.8 (4.9–2.1)	40.7 (44.4–37.1)
W33–35 asc2	—	—	—
A0–1 HCl	124 (1505–93)	4.1 (6.7–3.1)	129 (141–117)
A13–15 HCl	211 (695–156)	4.1 (5.7–3.3)	143 (152–134)
A39–41 HCl	44.6	3.1	139
W0–1 HCl	16.9	1.4	122
W13–15 HCl	29.4 (49.4–25.3)	2.34 (3.4–1.9)	132 (138–127)
W33–35 HCl	29.7 (73.3–25.8)	2.28 (4.1–1.8)	75.4 (80.8–70.0)

The parameter values are obtained by fitting the model to the time-dependent concentrations of ferrous iron in the extractions (Fig. 1). Upper and lower limits of the 95% confidence intervals are given in brackets.

Table 3
Total iron, phosphorus and calcium concentrations dissolved from the estuarine sediments in the chemical extractions after 24 h

	Iron (μmol/g dry sed) average ± standard deviation	Phosphorus (μmol/g dry sed) average ± standard deviation	Calcium (μmol/g dry sed) average ± standard deviation
A0–1 asc7	105.1 ± 1.0	74.4 ± 1.1	182.6 ± 6.8
A0–1 asc2	98.7 ± 0.6	44.2 ± 1.2	409.9 ± 9.3
A0–1 HCl	122.0 ± 3.1	48.4 ± 1.1	385.4 ± 11.4
A13–15 asc7	54.4 ± 3.0	43.2 ± 2.4	91.6 ± 4.7
A13–15 asc2	73.4 ± 1.4	40.1 ± 2.0	467.5 ± 13.7
A13–15 HCl	135.6 ± 0.8	57.7 ± 1.6	613.0 ± 18.5
A39–41 asc7	47.2 ± 1.1	38.8 ± 1.0	86.3 ± 2.4
A39–41 asc2	103.0 ± 1.4	48.4 ± 1.2	553.2 ± 12.2
A39–41 HCl	135.2 ± 4.9	51.4 ± 1.2	775.2 ± 58.9
W0–1 asc7	37.2 ± 0.9	10.9 ± 0.4	188.6 ± 8.0
W0–1 asc2	79.5 ± 2.4	15.1 ± 0.4	1580.1 ± 38
W0–1 HCl	124.3 ± 0.3	23.8 ± 0.1	>2000[a]
W13–15 asc7	19.1 ± 0.5	7.7 ± 0.3	154.0 ± 4.4
W13–15 asc2	40.0 ± 0.5	9.5 ± 0.5	1670.0 ± 62
W13–15 HCl	134.8 ± 1.7	19.3 ± 0.5	>2000[a]
W33–35 asc7	12.6 ± 0.5	6.6 ± 0.2	211.4 ± 6.8
W33–35 asc2	40.2 ± 3.2	7.5 ± 0.5	1437.0 ± 26
W33–35 HCl	79.0 ± 1.2	16.3 ± 0.03	>2000[a]

[a] Dissolved Ca concentrations already reached ⩾ 2.0 mmol/g dry sediment after 5 minutes and exceeded the maximum measurement standard after 24 h.

extractable by buffered ascorbate dropped by about 50% between the topmost sample and the two deeper samples, while the concentrations of HCl extractable iron remained approximately the same.

In buffered ascorbate–citrate solution, the time-dependent release of phosphorus and iron from the Appels sediments was characterized by a constant molar P/Fe ratio of 0.80 ± 0.05 during the 24 h of extraction (results not shown). Sediments from Waarde, however, did not exhibit such a stoichiometric release of P and Fe in buffered ascorbate–citrate solution: while initially P and F dissolved in a ratio close to 0.80, the release of P slowed down faster than that of Fe. For both Appels and Waarde sediments, the acid extractions (ascorbic acid and HCl), were characterized by an initial simultaneous release of both P and Fe, followed by continued dissolution of Fe, but little additional release of P (results not shown), resulting in lower P/Fe ratios at the end of the experiments compared to the buffered ascorbate extractions (Table 3).

The release of calcium increased in the order buffered ascorbate < ascorbic acid < HCl (Table 3). The effect was more pronounced at Waarde than at Appels. In all three extractant solutions, rapid initial releases of silicium and aluminium were followed by slower dissolution (results not shown). Significantly more Si and Al dissolved in 1 M HCl than in the ascorbate extractions. For comparison, after 24 h, the 1 M HCl, pH 2 ascorbic acid and pH 7.5 ascorbate extractions released 69–118, 9–22, 10–11 μmol Si per gram dry sediment, respectively. For Al, the corresponding concentrations were 47–80, 5–13, 2–10 μmol per gram dry sediment.

3.2. Microbial extractions

Little Fe^{2+} was generated in the control experiments with freeze-dried sediment suspended in sterile salt medium, whether or not lactate was added (Fig. 2). In the presence of *S. putrefaciens*, however, significant production of Fe^{2+} occurred. Without lactate addition, the final concentrations of ferrous iron in the suspensions with *S. putrefaciens* were on the order of 60% of those reached with lactate addition (Fig. 2). In one of the microbial incubations without added lactate (A0–1), ferrous iron production was accidentally interrupted due to contamination by ambient air.

Production of Fe^{2+} in sediment suspensions with *S. putrefaciens* and excess lactate increased linearly with time during at least the first 33 h of incubation (results not shown). The iron(III) reduction rates reported here were calculated from linear least square regressions of the measured ferrous iron concentrations (dissolved plus adsorbed) *versus* time, during the first 33 hours. The correlation coefficients (r^2) of the linear fits were always greater than 0.95.

For all six sediment intervals investigated, the iron(III) reduction rates by *S. putrefaciens* increased with increasing concentrations of sediment in the suspensions, although the rates leveled off for the highest sediment loadings. This saturation behavior can be seen in Fig. 3, where the rates are plotted against the initial concentrations of iron extractable by buffered ascorbate in the suspensions. Note that the rates in Fig. 3 are normalized by the number of cells in the incubations.

The saturation behavior of the iron(III) reduction rates with respect to Fe(III) substrate availability observed

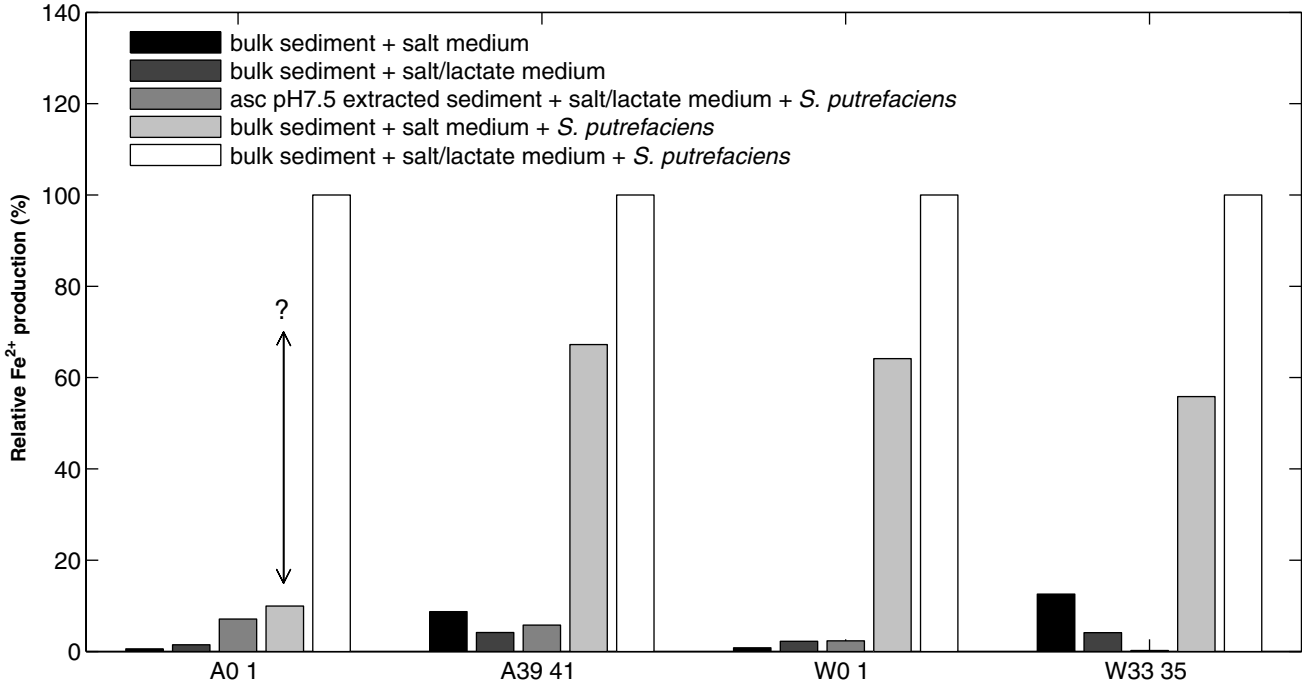

Fig. 2. Relative production of ferrous iron in the microbial incubations and controls, for the uppermost and deepest depth intervals of Appels and Waarde. For each depth interval, the Fe^{2+} production in the incubations with *S. putrefaciens* and excess lactate is set equal to 100%. The question mark indicates incomplete recovery of ferrous iron due to accidental introduction of air.

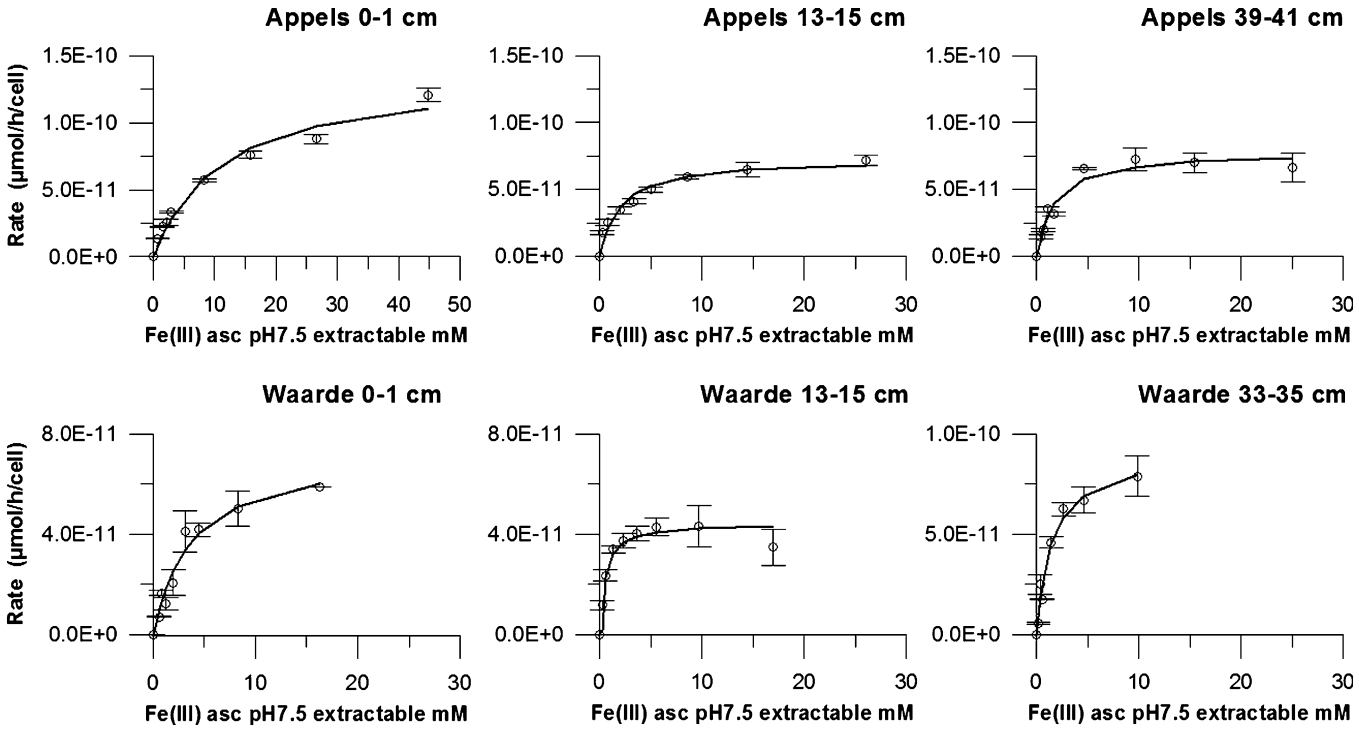

Fig. 3. Initial rates of iron reduction by *S. putrefaciens*, as a function of the concentrations of Fe(III) extractable by buffered ascorbate in the sediment-bacteria suspensions. Each data point on a plot corresponds to a different amount of sediment added to a fixed number of cells (2.1×10^{11} cells L^{-1}). Rates were determined from the Fe^{2+} build-up during the first 33 h of the microbial incubations. The lines are the best fits of Eq. (3) to the data.

here is similar to that reported by Bonneville et al. (2004) for the reduction of pure Fe(III) oxyhydroxides by *S. putrefaciens*. As proposed by these authors, the rates of ferrous iron production in the incubations with the natural sediments, R, were fitted to a Michaelis–Menten-type rate expression:

$$R = v_{\max} \cdot B \cdot \frac{[\mathrm{Fe(III)}]_{\mathrm{BA}}}{K_{\mathrm{m}} + [\mathrm{Fe(III)}]_{\mathrm{BA}}} \quad (3)$$

where v_{max} is the maximum Fe(III) reduction rate per cell, B the cell density per unit volume suspension, K_m an apparent affinity constant, and $[Fe(III)]_{BA}$ the concentration of iron extractable by buffered ascorbate–citrate solution, expressed per unit volume suspension. The best fits of Eq. (3) to the data are shown in Fig. 3, and the corresponding values of v_{max} and K_m are given in Table 4.

The maximum cell-specific rates of iron reduction by *S. putrefaciens* fell within a fairly narrow range. With the exception of the topmost sediment at Appels, v_{max} values ranged from 4.5×10^{-11} to 9.210^{-11} μmol h^{-1} $cell^{-1}$. For the uppermost centimeter of sediment at the freshwater site Appels, a higher maximum rate of 14.4×10^{-11} μmol h^{-1} $cell^{-1}$ was obtained. Note that the values of v_{max} are independent of how the Fe(III) substrate concentration is expressed.

In contrast, the apparent affinity constant K_m depends on the concentration units used for the Fe(III) substrate. For example, Table 4 compares K_m values expressed in units of concentration of iron extractable by buffered ascorbate–citrate solution (mmol Fe L^{-1}), and in units of mass dry sediment per unit of volume suspension (g L^{-1}). The former units are more relevant, because they directly relate to the availability of Fe(III) electron acceptor in the suspensions. As for v_{max}, with the exception of the uppermost sediment interval at Appels, values of K_m exhibited a rather narrow range, from 1.5 to 3.8 mmol Fe L^{-1}. For the 0–1 cm depth interval of Appels sediment, a higher value was found (11 mmol Fe L^{-1}).

The production of ferrous iron in the microbial incubations was strongly dependent on the cell to solid ratio. This is illustrated in Fig. 4, where the concentrations of ferrous

Table 4
Iron reduction of estuarine sediments by *S. putrefaciens*

	K_m g dry sediment L^{-1}	K_m mmol Fe(III) L^{-1}	v_{max} (10^{-11}) μmol Fe(III) h^{-1} $cell^{-1}$	$[Fe^{2+}]_{max}$ μmol g^{-1} dry sediment
A0–1	135 ± 30	11.1 ± 2.5	14.4 ± 1.4	66.4 ± 8.6
A13–15	41 ± 9	2.0 ± 0.4	7.3 ± 0.4	37.5 ± 3.1
A39–41	26 ± 8	2.0 ± 0.5	7.8 ± 0.4	25.2 ± 1.8
W0–1	89 ± 27	3.8 ± 0.9	7.4 ± 0.7	30.4 ± 0.8
W13–15	16 ± 3	0.30 ± 0.06	4.5 ± 0.2	17.6 ± 3.4
W33–35	75 ± 25	1.5 ± 0.3	9.2 ± 0.7	9.5 ± 0.9

The apparent half-saturation constants, K_m, and maximum cell-specific Fe(III) reduction rates, v_{max}, are obtained by fitting Eq. (3) to the initial iron reduction rates measured in the microbial incubations. The maximum concentrations of iron extractable by *S. putrefaciens*, $[Fe^{2+}]_{max}$, are derived from the best fits of Eq. (4) to the ferrous iron concentrations measured at the end of the microbial incubations. See text for complete discussion.

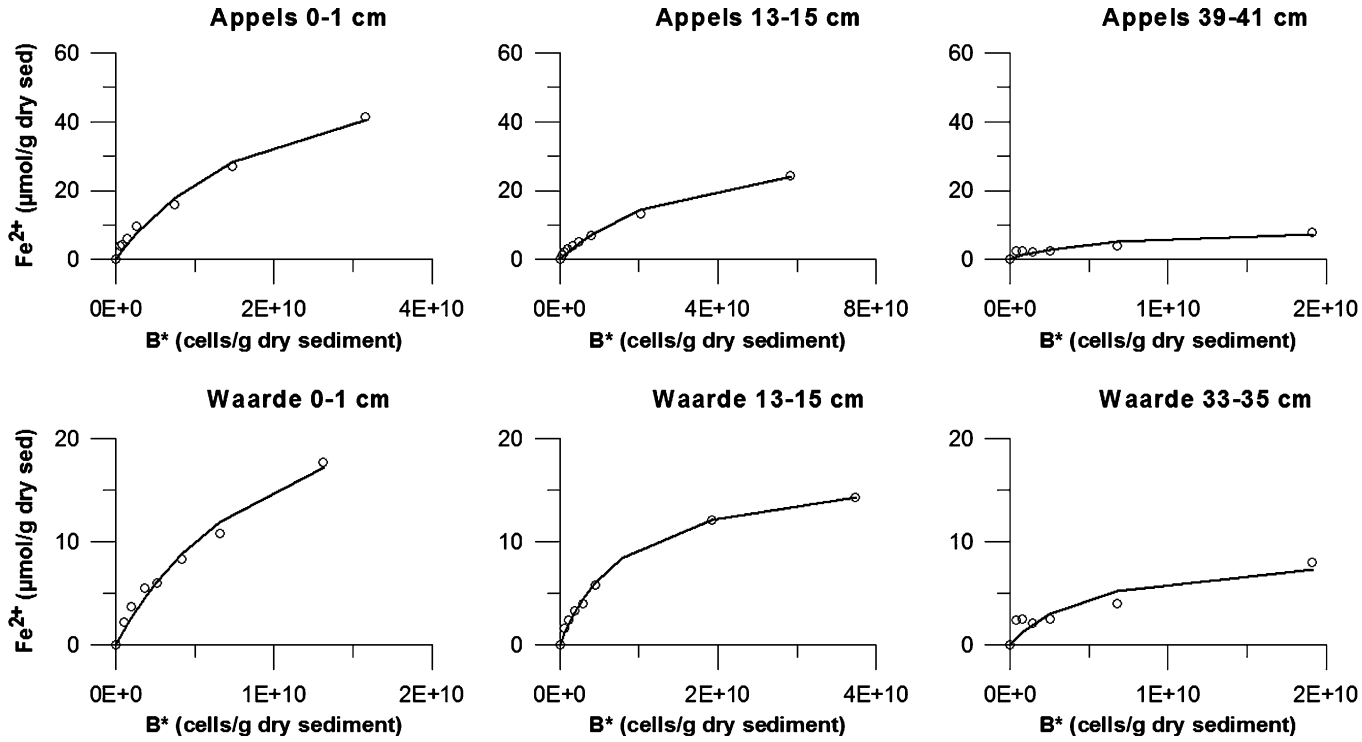

Fig. 4. Total ferrous iron produced in the microbial incubations after 600 h, as a function of the cell density per mass dry sediment, for the six sediment depth intervals. The lines are the best fits of Eq. (4) to the data.

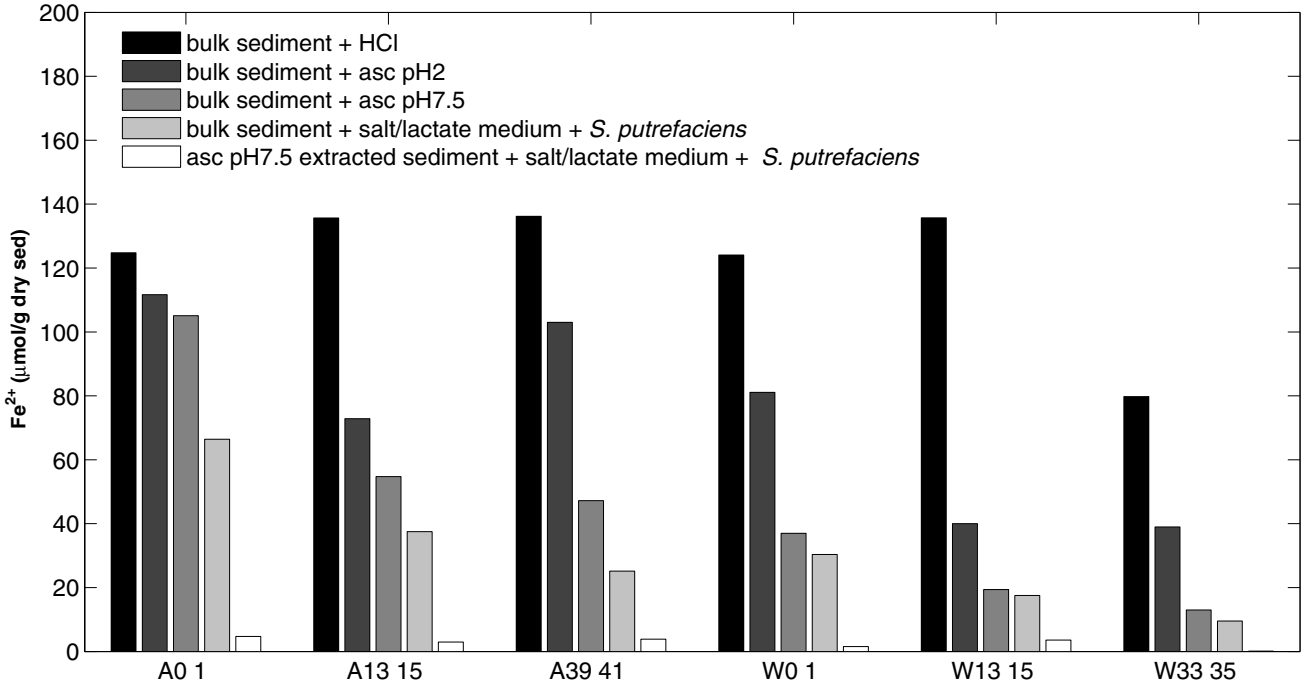

Fig. 5. Iron dissolution in chemical and microbial extractions. The iron concentrations for the chemical extractions correspond to the $M(0)$ values listed in Table 2, those for the microbial extractions are the maximum extractable concentrations of Fe(III) obtained from Eq. (4) ($[Fe^{2+}]_{max}$, see text and Fig. 4). The microbial extractions were performed with bulk, freeze-dried sediment, and with sediment pre-extracted with buffered ascorbate solution. See text for complete discussion.

iron measured at the end of the incubations (i.e., after 600 h) are plotted as a function of the cell density of *S. putrefaciens* per unit sediment mass. The observed parabolic shapes could be described by:

$$[Fe^{2+}] = [Fe^{2+}]_{max} \cdot \frac{B^*}{A + B^*} \quad (4)$$

where A is an adjustable fitting parameter, B^* the cell density per unit mass dry sediment, and $[Fe^{2+}]_{max}$ the asymptotic concentration of ferrous iron produced when the cell density is no longer limiting. Values of $[Fe^{2+}]_{max}$ were derived by fitting the data plotted in Fig. 4 to Eq. (4). The best-fit values of $[Fe^{2+}]_{max}$ are listed in Table 4.

In what follows, $[Fe^{2+}]_{max}$ is used as a measure of the microbially extractable Fe(III) initially present in the sediment. The highest value of $[Fe^{2+}]_{max}$ was observed in the uppermost depth interval of Appels sediment, the lowest in the deepest depth interval of Waarde sediment. For all depth intervals, $[Fe^{2+}]_{max}$ values were lower than the corresponding $M(0)$ values of the three chemical extractions (Fig. 5).

4. Discussion

4.1. Chemical extractions: kinetics

The three chemical extractions used in this study correspond to three different mechanisms of mineral dissolution in aqueous solution (Hering and Stumm, 1990). In buffered ascorbate–citrate solution, ascorbic acid and 1 M HCl, iron minerals undergo, respectively, ligand-enhanced reductive dissolution (Ferdelman, 1988; Kostka and Luther, 1994; Ferro, 2003; Hyacinthe and Van Cappellen, 2004), acid-enhanced reductive dissolution (Postma, 1993; Larsen and Postma, 2001; Roden, 2004), and proton-promoted dissolution (Chao and Zhou, 1983; Canfield, 1988; Svendsen et al., 1993; Raiswell et al., 1994).

Since the work of Postma (1993), the reactive continuum approach has been used to interpret the results of continuous chemical extractions of iron, manganese, phosphorus and silicate from natural sediments and aquifer materials (e.g., Koning et al., 1997; Ferro, 2003; Hyacinthe and Van Cappellen, 2004; van der Zee and van Raaphorst, 2004). The method consists in fitting the time-dependent release of the element of interest to Eq. (2). However, the applicability of the reactive continuum model depends on a number of factors, including the type of extractant and, hence, the dissolution mechanism, the nature and reactivity of the mineral phases undergoing dissolution, and the method of parameter estimation. These factors have not been critically assessed in previous studies.

The value of the apparent reaction order, $1 + 1/\upsilon$, and, consequently, its interpretation as a measure of the heterogeneity of the dissolving mineral assemblage, depends on the definition of the initial elemental mass, $M(0)$. The value assigned to $M(0)$ is critical, because the time-dependent variable being fitted by the continuum model is the relative change in extractable element mass, $M(t)/M(0)$. Therefore, comparison of kinetic parameters obtained in different

studies is only meaningful when the same definition of $M(0)$ is used.

In this study, we follow the approach of van der Zee and van Raaphorst (2004) by defining $M(0)$ as the maximum amount of iron a given extractant is able to dissolve from a particular sample. That is, the value of $M(0)$ is specific for the particular sample and extractant considered. As for a and υ, the value of $M(0)$ is derived from fitting Eq. (2) to the entire concentration time-series of a given extraction experiment. For the sediments and extractants used here, the fitted values of $M(0)$ are close to the aqueous iron concentrations measured after 24 h of extraction (Tables 2 and 3). This reflects the fact that the aqueous iron concentrations reach stable values before the end of the experiments. In other words, the three extraction solutions dissolve 100% of their corresponding $M(0)$ within 24 h.

Other authors operationally define $M(0)$ as the total amount of iron released by a more powerful extractant than the one used in the kinetic extraction. For example, Postma (1993) imposed the dithionite extractable iron concentration as $M(0)$, when fitting iron dissolution curves from sediments in ascorbic acid. Ferro (2003) applied the same method in her study of iron reactivity in estuarine sediments. Roden and Wetzel (2002) defined $M(0)$ as the iron extracted by 0.5 M HCl while modeling iron dissolution kinetics from freshwater sediments in pH 3 ascorbic acid.

With this second approach, the continuum model usually predicts incomplete dissolution at the end of a kinetic extraction experiment, because $M(0)$ includes a larger pool of iron phases than can be dissolved by the extractant under consideration. A major drawback is that when a large fraction of $M(0)$ remains undissolved at the end of the extraction, the model fits yield apparent reaction orders that are artificially high. Ferro (2003), for example, reports reaction orders in the range 4–19 (with an outlier of 68) for iron extractions in buffered ascorbate, compared to the generally lower values found here for similar estuarine sediments extracted identically (Table 2). Use of the extractant-specific value of $M(0)$ not only avoids the ambiguities associated with the operational definition of the total reactive iron content of a sample, but also those surrounding the interpretation of the corresponding reaction orders.

The results in Fig. 1 further show that the reactive continuum model fails to reproduce the observed shapes of the initial parts of the iron dissolution curves in the acid extraction media. As illustrated in Fig. 6, the pH 2 ascorbic acid and 1 M HCl extraction data are more consistent with the dissolution of distinct iron pools exhibiting vastly different reactivities, rather than with a reactive continuum.

The simulated dissolution curves in Fig. 6 assume 1:1 mixtures of two homogeneous iron pools. In the first case (Fig. 6A), the first-order dissolution rate constants differ by two orders of magnitude, in the second case (Fig. 6B) by one order of magnitude. In the latter simulation, the total iron dissolution curve is reasonably well reproduced by the reactive continuum model. Reducing the relative difference in rate constants further improves the model fits (results not shown). The same conclusion applies when more than two iron pools are included, as long as successive rate constants differ by one order of magnitude or less (results not shown). These findings are in line with those of Boudreau and Ruddick (1991), who assessed the applicability of the reactive continuum model to the early diagenetic degradation of organic matter.

When the dissolution rate constants in the mixture deviate by more than one order of magnitude, the reactive continuum model no longer matches the features of the dissolution curve (Fig. 6A). However, the deviations between the model and the dissolution curve in Fig. 6A resemble those observed for the pH 2 ascorbic acid and 1 M HCl extractions in Fig. 1. This suggests that the acid extractions release iron from (at least) two radically different sedimentary pools.

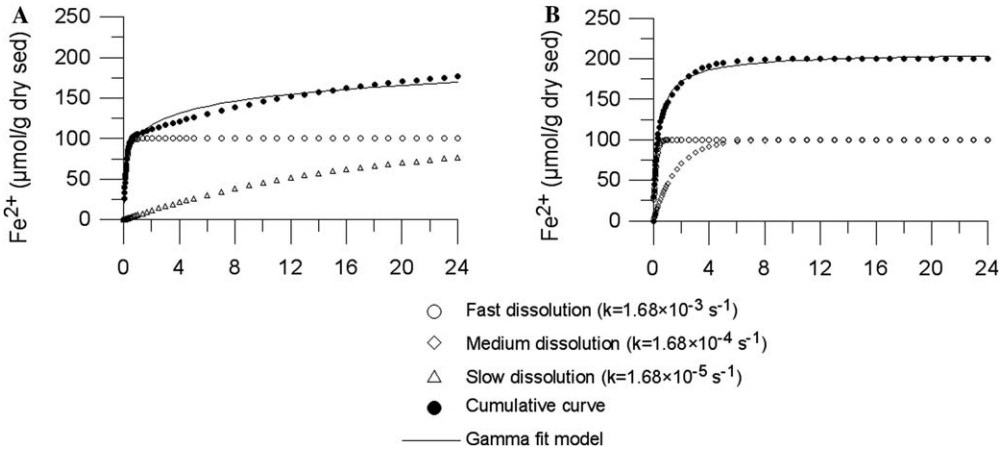

Fig. 6. Simulated iron dissolution curves for hypothetical 1:1 mixtures of two homogeneous iron mineral pools. Each pool follows first-order dissolution kinetics, characterized by a first-order rate constant, k. Two mixtures are considered, with rate constants differing by two (A) and one (B) order of magnitude, respectively. Dissolution curves are shown for the individual mineral pools and their mixtures. Solid lines are the best fits of the continuum model to the dissolution curves of the mixtures. See text for complete discussion.

The reactive continuum model has been used successfully in previous studies to fit iron dissolution curves during acid extractions (e.g., Postma, 1993; Larsen and Postma, 2001). Partly, this may reflect intrinsic differences in the nature and reactivity of the extracted iron phases. Another reason, of a more methodological nature, may also play an important role. The discrepancies between data and model reported here become apparent only because of the very high sampling resolution used, which, in particular, makes it possible to precisely define the very earliest portions of the dissolution curves. Previous studies have relied on coarser sampling intervals and the resulting data sets may, therefore, be insufficient to fully assess the validity of the reactive continuum model.

4.2. Chemical extractions: iron pools

The intertidal estuarine sediments used in this study are fairly rich in reactive iron: with the exception of the deepest sample at Waarde, the selected sediment intervals contain 1 M HCl extractable iron in excess of 0.5 weight %. In addition, our previous study provided evidence for intense redox cycling of iron at the two sites (Hyacinthe and Van Cappellen, 2004). Reduction of reactive Fe(III) phases was evident from the build-up of high pore water Fe^{2+} levels below the upper oxic layers of the sediments. At Waarde, the pore water Fe^{2+} profiles exhibited maxima at depths of 10–30 cm, below which they decreased because of aqueous Fe^{2+} removal by iron sulfide precipitation. Collection of authigenic precipitates on Teflon plates deployed at both sites further provided direct evidence for *in situ* oxidative precipitation of iron(III) within the uppermost few centimeters of the sediments and, at Waarde, also at greater depths around macrofaunal burrows (for a complete discussion, see Hyacinthe and Van Cappellen, 2004).

As can be seen in Fig. 5, the relative differences in the amounts of iron extracted by buffered ascorbate, ascorbic acid at pH 2 and 1 M HCl are much smaller for the top first centimeter of sediment at Appels, compared to the other five sediment intervals. These results indicate that the extracted iron in the upper oxidizing layer of the freshwater sediment consists mainly of a single pool of reducible Fe(III), which was previously identified as a hydrous ferric phosphate phase, with a molar P/Fe ratio in the range 0.7–0.8 (Hyacinthe and Van Cappellen, 2004).

The presence of ferric phosphate extractable by ascorbate–citrate solution at near-neutral pH was also demonstrated at the Waarde site. However, the time-dependent releases of Fe and P from Waarde sediments indicate that Fe(III) phases other than ferric phosphate are dissolved by the buffered ascorbate solution (Section 3.1). Presumably, these reducible iron phases are poorly crystalline iron(III) (hydr)oxides with P/Fe ratios well below 0.7 (Hyacinthe and Van Cappellen, 2004).

The significantly enhanced release of calcium during the acid extractions (Table 3) most likely reflects the non-reductive dissolution of minerals such as carbonates. The release of Si and Al further provides evidence for proton-promoted silicate mineral dissolution, especially in 1 M HCl (Section 3.1), while ferrous sulfide minerals are also known to dissolve under acid conditions (Cornwell and Morse, 1987). Thus, the acid extractions mobilize a broader range of distinctly different mineral constituents from the sediments, which explains why the reactive continuum model does not fit the iron dissolution curves by the acid extractants as well as those in buffered ascorbate–citrate solution.

Comparison of the three extractions indicate that reductive dissolution by ascorbate, at near-neutral pH and in the presence of citrate, is the most appropriate method to quantify the reactive Fe(III) pool in the estuarine sediments. As shown by Fig. 5, when *S. putrefaciens* cells are incubated with sediment previously treated with buffered ascorbate, no ferrous iron is produced. Hence, the buffered ascorbate extraction removes the bioavailable Fe(III) pool from the sediments.

4.3. Microbial extractions: kinetics

Bonneville et al. (2004) recently showed that, in the presence of excess lactate, initial reduction rates of pure, well-defined Fe(III) oxyhydroxides by *S. putrefaciens* exhibit saturation with respect to the availability of solid Fe(III) substrate. This behavior is described by the well-known Michaelis–Menten rate expression (Eq. (3)). The results in Fig. 3 show the same behavior for the set of iron-rich estuarine sediments studied here. Therefore, it should be instructive to compare the kinetic parameters v_{max} and K_m obtained for the natural sediments to those of the pure Fe(III) minerals.

The highest values of the maximum Fe(III) reduction rate per cell, v_{max}, were measured by Bonneville and coworkers for ferrihydrite ($8.1 \pm 0.3 \times 10^{-11}$ μmol h^{-1} $cell^{-1}$) and amorphous Fe(III) oxide ($6.5 \pm 0.3 \times 10^{11}$ μmol h^{-1} $cell^{-1}$), while a coarse-grained hematite yielded the lowest value ($0.27 \pm 0.03 \times 10^{11}$ μmol h^{-1} $cell^{-1}$). As can be seen in Table 4, with one exception, the v_{max} values for the natural sediments are similar, or higher, than those of ferrihydrite and amorphous Fe(III) oxide. Even the lowest v_{max} value, in sample W13–15, is only slightly smaller than that for synthetic amorphous Fe(III) oxide. The results thus imply that the sedimentary iron pool utilized by the bacteria consists of highly reactive Fe(III) phases.

A survey of available data further shows that the K_m values obtained for the estuarine sediments fall within the same order of magnitude as those for single reactive Fe(III) oxyhydroxides. For reduction by *S. putrefaciens* of ferrihydrite and amorphous ferric oxide suspensions, K_m values between 0.6 and 3 mM Fe(III) were found for a large range of mineral to bacteria ratios (Bonneville et al., 2004). With the exception of sample A0–1, similar values are obtained here (Table 4) when the buffered ascorbate extractable iron concentration is used as a measure of the bioavailable Fe(III) pool.

Roden and Wetzel (2002) and Jensen et al. (2003) found that microbial iron reduction in freshwater wetland sediments and nearshore marine sediments is no longer limited by the availability of reactive iron(III) phases at concentrations above 100 and 30 mmol Fe(III) L^{-1}, respectively. These results seem to imply higher K_m values than obtained here. A comparison between the studies is not straightforward, however, especially as different chemical extraction methods were used to assess the reactive iron(III) pools. Roden and Wetzel relied on HCl extractions. Jensen and coworkers used oxalate extractions, further correcting the extractable Fe(III) concentrations for the unreactive background levels. These authors also compared oxalate and HCl extractions and found that the latter overestimate bioavailable Fe(III). Thus, the corrected, oxalate-extractable Fe(III) concentrations of Jensen et al. are likely to reflect the reactive Fe(III) phases available to iron reducing organisms. The corresponding half-saturation constants (12 ± 5 mM Fe(III), Fig. 6 in Jensen et al., 2003) are in the upper range of our values (0.3–11.1 mM Fe(III), Table 4).

Half-saturation constants for in situ microbial iron reduction have also been constrained by reactive transport modeling (Wang and Van Cappellen, 1996). These authors fitted solid-state and pore water compositional depth profiles collected in three marine sediments of the Skagerrak using a multi-component early diagenetic model. To reproduce the observed reactive Fe(III) profiles, K_m values for dissimilatory iron reduction in the range 65–100 μmol Fe(III) g^{-1} dry sediment were required. These model-derived values are quite similar to the experimental values for Fe(III) reduction in estuarine sediments by *S. putrefaciens* (20–80 μmol Fe(III) g^{-1} dry sediment).

The relative magnitudes of the affinity constant, K_m, and the actual concentration of bioavailable Fe(III) determine whether or not microbial iron reduction is limited by Fe(III). Only when the concentration is significantly larger than K_m is the iron reduction rate independent of the availability of bioavailable Fe(III). On this account, the iron reducers in the six sediment depth intervals studied should be limited by the availability of reactive Fe(III). Limitation should be least severe in the uppermost depth interval at Appels, which contains the highest concentration of reactive Fe(III).

Maximum rates of microbial iron reduction reported for natural freshwater and marine sediments vary over several orders of magnitude (range 2–100 nmol Fe(III) cm^{-3} h^{-1}, Thamdrup, 2000; Roden and Wetzel, 2002; Jensen et al., 2003; Canavan et al., 2006). These rates are difficult to compare directly to cell-specific Fe(III) reductions rates such as those measured here for *S. putrefaciens*, because of a general lack of knowledge on the abundance, diversity and activity of iron reducers in sediments. This lack of knowledge represents a major stumbling block for the further development and calibration of kinetic models for *in situ* microbial iron reduction.

4.4. Chemical versus microbial extractions

In the buffered ascorbate extractions and the incubations with *S. putrefaciens* reactive Fe(III) mineral phases are reduced without the interference of proton-promoted dissolution processes. Both approaches indicate the presence of chemically and microbially reactive Fe(III) in all the sediments studied. They also concur that highly reactive and bioreducible Fe(III) is most abundant in the topmost sediment layer at the freshwater site. There are nonetheless some essential differences between the chemical extractions and the microbial incubations.

In particular, in the buffered ascorbate extractions Fe(III) is being reduced in the presence of excess reductant (ascorbate) and ligand (citrate). Hence, the rate at which iron is released does not depend explicitly on the concentrations of the reductant and ligand. In contrast, in the microbial incubations, the bulk iron reduction rate depends on the cell to sediment ratio (Fig. 4), indicating that saturation by the added bacterial biomass has not been reached.

Therefore, in order to compare chemically and microbially extractable Fe(III), we use the extrapolated, asymptotic ferrous iron concentration released by *S. putrefaciens*, $[Fe^{2+}]_{max}$ (Eq. (4), Fig. 4). The value of $[Fe^{2+}]_{max}$ is considered to represent the maximum amount of Fe(III) that can be reduced microbially, when biomass is present in excess and thus no longer limits the extent of Fe(III) reduction. These are the conditions most resembling those encountered in chemical extractions. In Fig. 7, the values of $[Fe^{2+}]_{max}$ are plotted against the corresponding values of $M(0)$ for the three types of chemical extractions performed.

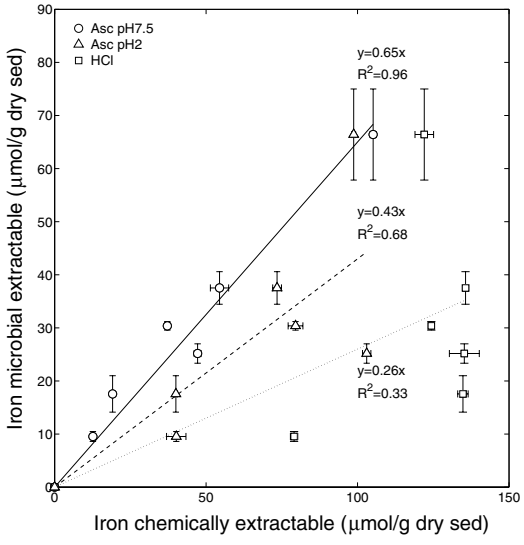

Fig. 7. Maximum concentrations of iron extractable by *S. putrefaciens* from the sediments ($[Fe^{2+}]_{max}$ in Eq. (4)) *versus* chemically extracted iron concentrations by the three extractant solutions ($M(0)$ in Eq. (1)). The solid, dashed and dotted lines are linear regressions of the data, forced through the origin for buffered ascorbate-citrate solution (pH 7.5), ascorbic acid (pH 2), and 1 M HCl, respectively.

The microbially extractable Fe(III) concentrations exhibit a strong linear correlation with the Fe(III) concentrations extracted by ascorbate-citrate solution at pH 7.5. This provides further evidence that the bacteria utilize the ascorbate reducible Fe(III) pool present in the sediments. Much weaker correlations are observed between $[Fe^{2+}]_{max}$ and iron release by the two other extraction solutions, with the lowest correlation coefficient for the 1 M HCl extractions. This is consistent with the mobilization by the acid extractions of (ferrous and ferric) iron phases that are not utilized by the bacteria.

The results in Fig. 7 also show that on average the bacteria only reduce 65% of the Fe(III) reducible by ascorbate. Apparently, the organisms are unable to access the remaining 35% of the reactive Fe(III) pool. Possibly, this is due to physical occlusion of a fraction of the reactive Fe(III) phases, as also suggested by Zachara et al. (2004) for a contaminated aquifer. Such a hypothesis is in line with our previous electron microscopic observations on the sediments (Hyacinthe and Van Cappellen, 2004). These reveal fine-grained, authigenic Fe(III) precipitates that are intimately associated with larger mineral grains. Thus, some of the precipitate mass may be located in small pores and cracks of the larger grains, where it can be reached by dissolved reactants, but not by the cells.

Because iron dissolution in buffered ascorbate solution follows the reactive continuum model, the apparent rate constant, υ/a, can be used as a relative measure of the chemical reactivity of the Fe(III) mineral phases undergoing reductive dissolution. Similarly, the maximum Fe(III) reduction rate per cell, v_{max}, provides a relative measure of the microbial reactivity of the sedimentary Fe(III). That is, variations in υ/a and v_{max} should reflect changes in the nature and properties of chemically and biologically reducible Fe(III) in the sediments. The two kinetic parameters are compared in Fig. 8.

The values of υ/a and v_{max} exhibit a rough correlation (Fig. 8). The significant scatter may in part be due to the relatively small ranges of parameter values for the set of sediments considered. A much stronger correlation emerges when including values of υ/a and v_{max} measured on single, synthetic Fe(III) mineral phases, covering a much broader range of chemical and microbial reactivities (Fig. 8). Specifically, lepidocrocite and coarse-grained hematite exhibit much lower values of υ/a and v_{max} than the sediments, while freshly precipitated ferric phosphate exhibits similar values. The high values of the kinetic parameters for the natural sediments confirm that *S. putrefaciens* utilizes the most reactive Fe(III) phases present in the sediments.

The correlations in Figs. 7 and 8 indicate a general correspondence between the kinetics and extent of iron mobilization in the microbial incubations and the extractions in buffered ascorbate–citrate solution. They also highlight some of the inherent caveats in using chemical extractions to infer the utilization of particulate Fe(III) by iron reducing microorganisms. In particular, the fraction of chemically reducible Fe(III) that is not accessible to microorganisms, because of physical occlusion, most likely varies from one sedimentary environment to another. Furthermore, some iron reducers may partially overcome this physical limitation by relying on dissolved electron shuttles (Royer et al., 2002; Kappler et al., 2004). Chemical extractions should therefore be used in conjunction with other methods in order to assess the potential for microbial iron reducing activity in natural porous media. These methods may include bioreduction experiments with model organisms, such as those performed here using *S. putrefaciens*, but also methods to characterize the distribution and fabric of iron mineral assemblages, plus the structure, physiology and activity of the resident iron reducing communities.

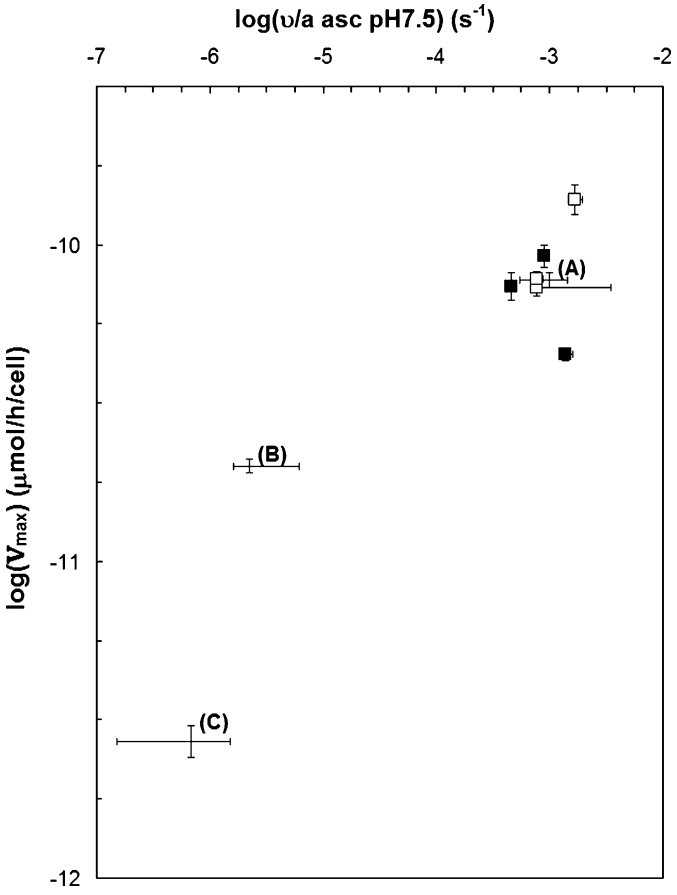

Fig. 8. Maximum iron reduction rates per cell (v_{max} in Eq. (3)) *versus* the apparent first-order rate constants for iron dissolution in buffered ascorbate solution (υ/a in Eq. (1)). Open (Appels) and filled (Waarde) squares correspond to the estuarine sediments, while (A), (B) and (C) indicate the ranges of the kinetic parameters for amorphous ferric phosphate, lepidocrite and hematite, respectively. The v_{max} values of the pure mineral phases were obtained following the procedure of Bonneville et al. (2004).

5. Conclusions

Extractions by ascorbate at near-neutral pH, in the presence of citrate as complexing agent, selectively mobilizes the reactive pool of reducible Fe(III) from the estuarine

sediments, within less than 24 h. The other two chemical extractions (pH 2 ascorbic acid and 1 M HCl) cause additional, acid-enhanced dissolution of ferrous iron minerals and significantly less reactive Fe(III) minerals. As a corollary, only the time-dependent dissolution of iron in the buffered ascorbate extractions is adequately described by the reactive continuum model.

The maximum concentrations of Fe(III) extractable by *S. putrefaciens* correlate linearly with the Fe(III) concentrations extracted in the buffered ascorbate–citrate extractions, implying that the bacteria utilize the ascorbate reducible Fe(III) pool of the sediments. The maximum iron reduction rates per cell, v_{max}, obtained for the estuarine sediments are of comparable magnitude as those measured for ferrihydrite and amorphous ferric oxide reduction by *S. putrefaciens*. The values of v_{max} for the sediments and pure Fe(III) mineral phases further correlate positively with the apparent first-order rate constants of iron reduction in buffered ascorbate–citrate solution.

The incomplete utilization by *S. putrefaciens* of the ascorbate reducible pool of Fe(III) indicates that physical access of solid-phase Fe(III) may potentially be a limiting factor for *in situ* dissimilatory iron reduction. The enhanced accessibility to sedimentary Fe(III) phases of dissolved reactants (e.g., ascorbate and citrate), relative to the much larger cells of iron reducing bacteria, represents a significant difference between chemical and microbial extractions. The buffered ascorbate extractable Fe(III) concentrations therefore provide maximum estimates of the bioavailable Fe(III) present in the sediments.

Acknowledgments

The authors acknowledge the constructive comments and suggestions of Rob Raiswell, two anonymous reviewers and the Associate Editor, David Burdige. This study was financially supported by the Netherlands Organisation for Scientific Research through an NWO Pioneer Grant, and by the Centre for Soil Quality Management and Knowledge Transfer (SKB), Delft Cluster (DC) and NWO through TRIAS Project 835.80.004.

Associate editor: David J. Burdige

References

Baeyens, W., van Eck, B., Lambert, C., Wollast, R., Goeyens, L., 1998. General description of the Scheldt estuary. *Hydrobiologia* **366**, 1–14.

Bertani, G., 1951. Studies on lysogenesis. I. The mode of phage liberation by lysogenic *Escherichia coli*. *J. Bacteriol.* **62**, 293–300.

Bonneville, S., Van Cappellen, P., Behrends, T., 2004. Microbial reduction of iron(III) oxyhydroxides: effects of mineral solubility and availability. *Chem. Geol.* **212**, 255–268.

Bordas, F., Bourg, A.C.M., 1998. A critical evaluation of samples preatreatment for storage of contaminated sediments to be investigated for the potential mobility of their heavy metal load. *Water Air Soil Pollut.* **103**, 137–149.

Boudreau, B.P., Ruddick, B.R., 1991. On a reactive continuum representation of organic matter diagenesis. *Am. J. Sci.* **291**, 507–538.

Buffle, J., de Vitre, R.R., Perret, D., Leppard, G.G., 1989. Physicochemical characteristics of a colloidal iron phosphate species formed at the oxic-anoxic interface of a eutrophic lake. *Geochim. Cosmochim. Acta* **53**, 399–408.

Canavan, R.W., Slomp, C.P., Jaroubchi, P., Van Cappellen, P., Laverman, A., van den Berg, G.A., 2006. Organic matter mineralization of a coastal freshwater lake and response to salinization. *Geochim. Cosmochim. Acta* **70**, 2836–2855.

Canfield, D.E., 1988. Sulfate reduction and the diagenesis of iron in anoxic marine sediment. PhD Thesis, Yale University.

Canfield, D.E., 1993. Organic matter oxidation in marine sediments. In: Wollast, R., Mackenzie, F.T., Chou, L. (Eds.), *Interactions of C, N, P and S Biogeochemical Cycles and Global Change*. Springer-Verlag, New-York, pp. 333–363.

Chao, T.T., Zhou, L., 1983. Extraction techniques for selective dissolution of amorphous iron oxides from soils and sediments. *Soil Sci. Soc. Am. J.* **47**, 225–232.

Chen, J., Gu, B., Royer, R.A., Burgos, W.D., 2003. The roles of natural organic matter in chemical and microbial reduction of ferric iron. *Sci. Total Environ.* **307**, 167–178.

Cornwell, J.C., Morse, J.W., 1987. The characterization of iron sulfide minerals in marine sediments. *Mar. Chem.* **22**, 193–206.

DiChristina, T.J., DeLong, E.F., 1994. Isolation of anaerobic respiratory mutants of *Shewanella putrefaciens* and genetic analysis of mutants deficient in anaerobic growth on Fe^{3+}. *J. Bacteriol.* **176**, 1468–1474.

DiChristina, T.J., Moore, C.M., Haller, C.A., 2002. Dissimilatory Fe(III) and Mn(IV) reduction by *Shewanella putrefaciens* requires ferE, a homolog of the pulE (gspE) type II protein secretion gene. *J. Bacteriol.* **184**, 142–151.

Dollhopf, M.E., Nealson, K.H., Simon, D.M., Luther III, G.W., 2000. Kinetics of Fe(III) and Mn(IV) reduction by the Black Sea strain of *Shewanella putrefaciens* using in situ solid state voltammetric Au/Hg electrodes. *Mar. Chem.* **70**, 171–180.

Dos Santos Afonso, M., Morando, P.J., Blesa, M.A., Banwart, S., Stumm, W., 1990. The reductive dissolution of iron oxides by ascorbate. *J. Coll. Interface Sci.* **138**, 74–82.

Ferdelman, T.G., 1988. The distribution of sulfur, iron, manganese, copper and uranium in a salt marsh sediment core by a sequential extraction method. MSc. Thesis, Delaware University.

Ferro, I., 2003. Cycling of iron and manganese in freshwater, estuarine and deep sediment. PhD thesis, Groningen University.

Fredrickson, J.K., Zachara, J.M., Kennedy, D.W., Dong, H., Onstott, T.C., Hinman, N.W., Li, S.-M., 1998. Biogenic iron mineralization accompanying the dissimilatory reduction of hydrous ferric oxide by a groundwater bacterium—sorption of Mn^{2+} on $FeCO_3$. *Geochim. Cosmochim. Acta* **62**, 3239–3257.

Froelich, P.N., Klinkhammer, G.P., Bender, M.L., Luedtke, N.A., Heath, G.R., Cullen, D., Dauphin, P., Hammond, D., Hartman, B., Maynard, V., 1979. Early oxidation of organic matter in pelagic sediments of the eastern equatorial Atlantic: suboxic diagenesis. *Geochim. Cosmochim. Acta* **43**, 1075–1090.

Hacherl, E.L., Kosson, D.S., Young, L.Y., Cowan, R.M., 2001. Measurement of Iron(III) bioavailability in pure iron oxide minerals and soils using anthraquinone-2,6-disulfonate oxidation. *Environ. Sci. Technol.* **35**, 4886–4893.

Haese, R.R., Petermann, H., Dittert, L., Schulz, H.D., 1998. The early diagenesis of iron in pelagic sediments: a multidisciplinary approach. *Earth Planet. Sci. Lett.* **157**, 233–248.

Hering, J.G., Stumm, W., 1990. Oxidative and reductive dissolution of minerals. In: Hochella, M.F., White A.F., (Ed.), Mineral-Water Interface Geochemistry, Vol. 23. pp. 427-465.

Hobbie, J.E., Daley, R.J., Jasper, S., 1977. Use of nucleopore filters for counting bacteria by fluorescence microscopy. *Appl. Environ. Microbiol.* **33**, 1225–1228.

Hyacinthe, C., Van Cappellen, P., 2004. An authigenic iron phosphate phase in estuarine sediments: composition, formation and chemical reactivity. *Mar. Chem.* **91**, 227–251.

Jensen, M.M., Thamdrup, B., Rysgaard, S., Holmer, M., Fossing, H., 2003. Rates and regulation of microbial iron reduction in sediments of Baltic-North Sea transition. *Biogeochemistry* **65**, 295–317.

Jones, J.G., Gardener, S., Simon, B.M., 1983. Bacterial reduction of ferric iron in a stratified eutrophic lake. *J. Gen. Microbiol.* **129**, 131–139.

Jones, J.G., Davison, W., Gardener, S., 1984. Iron reduction by bacteria: range of organisms involved and metals reduced. *FEMS Microbiol. Lett.* **21**, 133–136.

Kappler, A., Benz, M., Schink, B., Brune, A., 2004. Electron shuttling via humic acids in microbial iron(III) reduction in a freshwater sediment. *FEMS Microbiol. Ecol.* **47**, 85–92.

Koning, E., Brummer, G.-J., Van Raaphorst, W., Van Bennekom, J., Helder, W., Van Iperen, J., 1997. Settling, dissolution and burial of biogenic silica in the sediments off Somalia (northwestern Indian Ocean). *Deep Sea Res. II* **44**, 1341–1360.

Kostka, J.E., Haefele, E., Viehweger, R., Stucki, J.W., 1999. Respiration and dissolution of iron(III)-containing clay minerals by bacteria. *Environ. Sci. Technol.* **33**, 3127–3133.

Kostka, J.E., Luther III, G.W., 1994. Partitioning and speciation of solid phase iron in saltmarsh sediments. *Geochim. Cosmochim. Acta* **58**, 1701–1710.

Larsen, O., Postma, D., 2001. Kinetics of reductive bulk dissolution of lepidocrocite, ferrihydrite, and goethite. *Geochim. Cosmochim. Acta* **65**, 1367–1379.

Lin, B., 2006. Composition and functioning of iron-reducing communities in two constrasting environments, i.e., a landfill leachate-polluted aquifer and estuarine sediments. Ph.D. Thesis, Free University of Amsterdam.

Lovley, D.R., Phillips, E.J.P., 1986a. Availability of ferric iron for microbial reduction in bottom sediments of freshwater tidal Potomac river. *Appl. Environ. Microbiol.* **52**, 751–757.

Lovley, D.R., Phillips, E.J.P., 1986b. Organic matter mineralization with reduction of ferric iron in anaerobic sediments. *Appl. Environ. Microbiol.* **51**, 683–689.

Lovley, D.R., Phillips, E.J.P., 1988. Novel mode of microbial energy metabolism: organic carbon oxidation coupled to dissimilatory reduction of iron or manganese. *Appl. Environ. Microbiol.* **54**, 1472–1480.

Murray, J.W., 1979. Iron oxides. In: Burns, R.G. (Ed.), *Marine Minerals*. Mineralogical Society of America, Washington DC, pp. 47–97.

Nealson, K.H., Saffarini, D., 1994. Iron and manganese in anaerobic respiration: environmental significance, physiology, and regulation. *Annu. Rev. Microbiol.* **48**, 311–343.

Postma, D., 1993. The reactivity of iron oxides in sediments: a kinetic approach. *Geochim. Cosmochim. Acta* **57**, 5027–5034.

Poulton, S.W., Raiswell, R., 2005. Chemical and physical characteristics of iron oxides in riverine and glacial meltwater sediments. *Chem. Geol.* **218**, 203–221.

Raiswell, R., Canfield, D.E., 1998. Sources of iron for pyrite formation in marine sediments. *Am. J. Sci.* **298**, 219–245.

Raiswell, R., Canfield, D.E., Berner, R.A., 1994. A comparison of iron extraction methods for the determination of degree of pyritization and the recognition of iron-limited pyrite formation. *Chem. Geol.* **111**, 101–110.

Roden, E.E., Wetzel, R.G., 2002. Kinetics of microbial Fe(III) oxide reduction in freshwater wetland sediments. *Limnol. Oceanogr.* **47**, 198–211.

Roden, E.E., 2004. Analysis of long-term bacterial vs. chemical Fe(III) oxide reduction kinetics. *Geochim. Cosmochim. Acta* **68**, 3205–3216.

Roden, E.E., Wetzel, R.G., 1996. Organic carbon oxidation and suppression of methane production by microbial Fe(III) oxide reduction in vegetated and unvegetated freshwater wetland sediments. *Limnol. Oceanogr.* **41**, 1733–1748.

Royer, R.A., Burgos, W.D., Fisher, A.S., Unz, R.F., Dempsey, B.A., 2002. Enhancement of biological reduction of hematite by electron shuttling and Fe(II) complexation. *Environ. Sci. Technol.* **36**, 1939–1946.

Schwertmann, U., Cornell, R.M., 1991. *Iron oxides in the laboratory*. VCH, Weinheim.

Slomp, C.P., Malschaert, J.F.P., Lohse, L., van Raaphorst, W., 1997. Iron and manganese cycling in different sedimentary environments on the North Sea continental margin. *Cont. Shelf Res.* **17**, 1083–1117.

Sorensen, J., 1982. Reduction of ferric iron in anaerobic, marine sediment and interaction with reduction of nitrate and sulfate. *Appl. Environ. Microbiol.* **43**, 319–324.

Stookey, L.L., 1970. Ferrozine—A new spectrophotometric reagent for iron. *Anal. Chem.* **42**, 779–781.

Stumm, W., Sulzberger, B., 1992. The cycling of iron in natural environments: consideration based on laboratory studies of heterogneous redox processes. *Geochim. Cosmochim. Acta* **56**, 3233–3257.

Svendsen, L.M., Rebsdorf, A., Nornberg, P., 1993. Comparison of methods for analysis of organic and inorganic phosphorus in river sediment. *Water Res.* **27**, 77–83.

Thamdrup, B., 2000. Microbial manganese and iron reduction in aquatic sediments. In: Schink, B. (Ed.), *Advances in Microbial Ecology*. Kluwer, New York, pp. 41–84.

Thamdrup, B., Fossing, H., Jorgensen, B.B., 1994. Manganese, iron, and sulfur cycling in a coastal marine sediment, Aarhus Bay, Denmark. *Geochim. Cosmochim. Acta* **58**, 5115–5129.

van der Zee, C., 2002. Early diagenesis of manganese, iron and phosphorus in european continental margin sediments. Ph. D. thesis, Utrecht Univ.

van der Zee, C., van Raaphorst, W., 2004. Manganese oxide reactivity in North Sea sediments. *J. Sea Res.* **52**, 73–85.

Viollier, E., Inglett, P.W., Hunter, K., Roychoudhury, A.N., Van Cappellen, P., 2000. The ferrozine method revisited: Fe(II)/Fe(III) determination in natural waters. *Appl. Geochem.* **15**, 785–790.

Wang, Y., Van Cappellen, P., 1996. A multicomponent reactive transport model of early diagenesis: application to redox cycling in coastal marine sediments. *Geochim. Cosmochim. Acta* **60**, 2993–3014.

Wollast, R., 1988. The Scheldt estuary. In: Salomons, W., Blayne, B.L., Duursma, E.K., Forstmer, U. (Eds.), *Pollution of the North Sea: An Assessment*. Springer, Berlin, pp. 183–193.

Zachara, J.M., Fredrickson, J.K., Li, S.-M., Kennedy, D.W., Smith, S.C., Gassman, P.L., 1998. Bacterial reduction of crystalline Fe^{3+} oxides in single phase suspension and subsurface materials. *Am. Mineral.* **83**, 1426–1443.

Zachara, J.M., Kukkadapu, R.K., Gassman, P.L., Dohnalkova, A., Fredrickson, J.K., Anderson, T., 2004. Biogeochemical transformation of Fe minerals in a petroleum-contaminated aquifer. *Geochim. Cosmochim. Acta* **68**, 1691–1700.